Long Non-Coding RNA ADAMTS9-AS1 Represses Ferroptosis of Endometrial Stromal Cells Through Regulating miR-6516-5p/GPX4 Axis in Endometriosis

Yiting Wan
Shanghai municipal Hospital of Traditional Chinese Medicine, Shanghai University of Traditional Chinese Medicine

Cancan Gu
Shanghai municipal Hospital of Traditional Chinese Medicine, Shanghai University of Traditional Chinese Medicine

Jueying Kong
Shanghai municipal Hospital of Traditional Chinese Medicine, Shanghai University of Traditional Chinese Medicine

Jin Sui
Shanghai municipal Hospital of Traditional Chinese Medicine, Shanghai University of Traditional Chinese Medicine

Ling Zuo
Shanghai municipal Hospital of Traditional Chinese Medicine, Shanghai University of Traditional Chinese Medicine

Yanhua Song
Shanghai municipal Hospital of Traditional Chinese Medicine, Shanghai University of Traditional Chinese Medicine

Jing Chen (cj1275@126.com)
Shanghai municipal Hospital of Traditional Chinese Medicine, Shanghai University of Traditional Chinese Medicine

---

Research Article

Keywords: Endometriosis, ADAMTS9-AS1, miR-6516-5p, GPX4, ferroptosis

Posted Date: August 2nd, 2021

DOI: https://doi.org/10.21203/rs.3.rs-737739/v1

Abstract

Endometriosis (EMs) is one of the most frequent diseases in reproductive age women, characterized by the growth of endometrial tissues beyond the uterus. Enhanced proliferative and migratory potential of endometrial stromal cells (ESCs) is the major cause of EMs. Mounting studies have demonstrated that long non-coding RNAs (lncRNAs) exert an important role in regulating the development and progression of EMs. Given the aberrant expression of lncRNA ADAMTS9-AS1 in ectopic endometrium (ecEM), here we investigated the biological effect of ADAMTS9-AS1 on ESCs proliferation and migration and explored the underlying mechanism. The current data showed that the ADAMTS9-AS1 expression was significantly up-regulated in ecEM compared with eutopic endometrium (euEM) in patients with EMs and in a murine model of EMs. Functionally, ADAMTS9-AS1 knockdown in ectopic ESCs (EESCs) decreased cell viability and migration, whereas ADAMTS9-AS1 overexpression in normal ESCs (NESCs) enhanced cell viability and migration. More important, the effect of ADAMTS9-AS1 inhibition on decreasing ESCs viability was significantly blocked by Ferrostatin-1 (Fer-1, a ferroptosis inhibitor), and ADAMTS9-AS1 overexpression repressed Erastin (a ferroptosis activator)-induced cell death. Furthermore, the regulatory role of ADAMTS9-AS1 in ferroptosis was defined and evidenced by increased reactive oxygen species (ROS) level and malonyl dialdehyde (MDA) content, and decreased expression of glutathione peroxidase 4 (GPX4) after ADAMTS9-AS1 inhibition. Mechanistically, ADAMTS9-AS1 functioned as a competing endogenous RNA (ceRNA) via sponging miR-6516-5p to de-repress the expression of GPX4, the critical repressor of ferroptosis. Taken together, these results demonstrate that up-regulated ADAMTS9-AS1 accelerates ESCs proliferation and migration through regulating miR-6516-5p/GPX4-dependent ferroptosis, and may be a potential target for the treatment of EMs.

Introduction

Endometriosis (EMs) is a common and polyfactorial disorder in which environmental, genetic, immunologic, and hormonal aberrations are correlated with the pathological process of EMs (1, 2). EMs is characterized by the growth of histologically normal endometrial tissues beyond the uterus, and affects between 10%-15% women of fertile age worldwide (3, 4). The major clinical manifestations of EMs include infertility, chronic pelvic pain and vaginal bleeding, and thus negatively affect these woman's life quality. Recently, mounting experimental evidence demonstrated that non-coding RNAs (ncRNAs) act as an importantly regulatory role in the pathogenesis of EMs and in the EMs-associated symptoms (5, 6).

Long non-coding RNA (LncRNA) is a kind of RNA molecules with the length of more than 200 nt that does not possess a protein-coding potential (7). Mounting studies suggested that the dys-regulated lncRNA expression is closely correlated with a variety of biological processes and human diseases, such as Chromosome dose compensation, development, tumorigenesis, and cardiovascular diseases (8–11). For example, Xu *et al*., reported that 172 lncRNAs and 188 mRNAs are differentially expressed in endometrial carcinoma tissues compared with normal tissues (12). Several lncRNAs (KIAA0087, RP11-501O2, FAM212B-AS1, etc.) might be key regulator to endometrial carcinogenesis and progression. Emerging evidence has also revealed the role lncRNAs in the pathogenesis of EMs. A total of 576 differentially

expressed lncRNAs are identified in ectopic endometrium of adenomyosis, of which 388 lncRNAs are increased and 188 lncRNAs are decreased (13). Zhang *et al*., demonstrated that the expression of lncRNA CCDC144NL-AS1 expression is upregulated in ectopic endometrial tissues compared with paired eutopic endometrial and normal endometrial (NE) tissues (14). Functional studies further showed that CCDC144NL-AS1 inhibition decreases endometrial stromal cells (ESCs) migration and invasion (14).

The role of lncRNA ADAMTS9-AS1 (thereafter named ADAMTS9-AS1) in tumor progression has been widely investigated. Low expression of ADAMTS9-AS1 predicts a poorer survival compared with higher ADAMTS9-AS1 expression in patients with prostate cancer, and ADAMTS9-AS1 inhibits prostate cancer cell proliferation, indicating that ADAMTS9-AS1 functions as a tumor suppressive role in prostate cancer (15). A recent study showed that ADAMTS9-AS1 is significantly increased in ectopic endometrial tissues (16). However, the biological role of ADAMTS9-AS1 in EMs remains unknown.

Ferroptosis is an iron-dependent non-apoptotic cell death and distinctly differ from other forms of cell death including apoptosis, pyroptosis, senescence and autophagy (17–20). Overproduction of iron-induced lipid reactive oxygen species (ROS) is the crucial event in ferroptosis (21, 22). Although the levels of iron and lipid peroxide content are increased in the peritoneal fluid of women with EMS compared to those without (23–25), the role of ferroptosis in EMs has not been systematically investigated. In the study we demonstrated that ADAMTS9-AS1 was significantly up-regulated in ecEM compared with euEM. ADAMTS9-AS1 knockdown decreased cell viability and migration, whereas the effect was blocked by ferroptosis inhibitor. ADAMTS9-AS1 functioned as a ceRNA via sponging miR-6516-5p to de-repress the expression of GPX4.

Materials And Methods

A murine model of EMs

Animal experiments were approved by the Experimental Animal Committee of Shanghai municipal Hospital of Traditional Chinese Medicine, and carried out according to Shanghai municipal Hospital of Traditional Chinese Medicine guidelines for the use of animals. All animal experiments were performed in accordance with the ARRIVE guidelines as described previously (26) to minimize the animals number used in the study and suffering of the animal. The female BALB/c mice (4-6 weeks old, 18-20 g) were obtained from the Shanghai Regan Biotechnology Co., Ltd (Shanghai, China) and were reared in a specific, pathogen-free facility. (27-29). After 1-week acclimatization, mice were randomly divided into two groups: the donor group (n=10) and recipient groups (n=10). Ovariosteresis and estradiol valerat-injection (0.5 μg/mouse/week; Aladdin, Shanghai, China) was carried out to avoid differences of oestrous cycle (28). Mice were anesthetized by 2% isoflurane and then ovaries on both sides were exposed through flank incisions and removed. Donor mice were sacrificed under isoflurane anesthesia and each uterine horn of donor mice was concentrated and peeled in warm PBS to remove uterine muscle. Endometrium tissues were weight and cut into small fragments with scissors and resuspended in sterile PBS with 1× ampicillin (Beyotime, Shanghai, China). After that, endometrium preparation was intraperitoneally

injected into two recipient mice (50 mg/mice). Two weeks after EM transplant, endometriosis lesions and eutopic endometrium tissues were removed from the peritoneal cavities and uteri.

Clinical samples

Human ectopic and eutopic endometrium tissues (n=17) were provided by Shanghai municipal Hospital of Traditional Chinese Medicine with written informed consent signed by the patients according to Declaration of Helsinki Principles. All of the protocols in this study is approved by Shanghai municipal Hospital of Traditional Chinese Medicine.

Primary ESCs

Primary murine ESCs were isolated from eutopic and ectopic endometrium tissues of recipient mice. Briefly, endometrium tissues were wash with PBS and minced into small fragments, then treat with 0.3% collagenase I and 0.01% trypsin (Sigma-Aldrich, MO, USA) in DMEM/12F medium (Sigma-Aldrich) for 50 min at 37 °C, followed by filtration through 100 μm and 70 μm nylon cell strainers. All cells were maintained in DMEM/F-12 with 10% fetal bovine serum (Thermo fisher Scientific, DE, USA) and 1× Penicillin-Streptomycin (Beyotime, Shanghai, China) at 37°C under humidified 5% CO_2.

Total RNA extraction and quantitative RT-PCR (qPCR) assay

Total RNA was extracted from endometrial tissues or ESCs with RNAiso Plus (TaKaRa Bio Inc., Otsu, Shiga, Japan) according to the manufacturer's instructions, quantitated by Multiskan SkyHigh (Thermofisher Scientific). Prime Script RT-PCR Kit (TaKaRa) was applied to carry out reverse transcription PCR (RT-PCR). The RT-PCR protocol was 65˚C for 5 min, 30 ˚C for 10 min, and 42˚C for 30 min. qPCR was performed using Accurate 96 (DLAB, China) with ChamQ Universal SYBR qPCR Master Mix (Vazyme, Nanjing, China). The program setting was based on the manufacturer's recommendations, thermocycling conditions were as follows: initial denaturation at 95 °C for 10 s, denaturation at 95 °C for 10 s, annealing and extension at 65 °C for 10 s; the reaction was performed for 30 cycles. Each reaction was carried out at least in triplicate. ADAMTS9-AS1 and GPX4 RNA transcriptions were quantified by the $2^{-\Delta\Delta Ct}$ method and normalized by endogenous β-actin mRNA. The primer sequences were listed in Supporting Table S1.

Overexpression and RNA interference (RNAi)

The recombinant construct (pcDNA-ADAMTS9-AS1) containing full-length ADAMTS9-AS1 sequence was constructed by inserting their open reading frame into the pcDNA vector. miR-6516-5p mimics were used to mimic the overexpression of miR-6516-5p. siRNA-ADAMTS9-AS1 (siADAMTS9-AS1) was used to knockdown ADAMTS9-AS1 in ESCs and siRNA-control (N.C) was used as a control. The ESCs were seeded into culture dishes before transfection, until the cells adhered on the second day. Lipofectamine™ 3000 (Invitrogen, Carlsbad, CA, USA) was applied to prepare the mixture of siADAMTS9-AS1, N.C, miR-6516-5p or pcDNA-ADAMTS9-AS1 with Lipofectamine™ 3000 according to the instructions.

Cell viability assay

The cell viability of NESCs and EESCs was determined with CCK-8 Cell Proliferation and Cytotoxicity Assay Kit (CCK-8; Solar Bio, Beijing, China) following the manufacturer's instructions. Before transfection or drug treatment, ESCs were seeded onto 96-well-plates at a density of 6 ´ 10^3 cells/well to incubate for 24 h. To explore the effect of ADAMTS9-AS1 on regulating ESCs viability and the pattern of ADAMTS9-AS1-induced ESCs cells death, ADAMTS9-AS1 in ESCs was knocked down or overexpressed in the present or absent of cell death inhibitors (Fer-1, 1 μM; ZVAD-FMK, 10 μM; necrostatin-1, 10 μM; 3-MA, 10 mM; and disulfiram, 5 μM) or inducer (Erastin, 10 μM; Sorafenib, 5 μM) purchased from Sigma-Aldrich (Shanghai, China). Then the cells were treated with 15 μL CCK-8 reagent and incubated for another 3 h at 37°C. The absorbance was measured at 450 nm with Multiskan SkyHigh (Thermofisher Scientific, Wilmington, DE, USA).

FDA staining was also performed to determine whether ADAMTS9-AS1 knockdown regulated cell death of EESCs. After being transfected with si-ADAMTS9-AS1 or siRNA-control for 48 hours, EESCs were treated with 100 μg/mL FDA (Thermofisher Scientific, Wilmington, DE, USA) and incubated in dark for 20 min, then observed by microscopy.

Transwell migration assay

To explore the effect of ADAMTS9 AS1 and miR-6516-5p on regulating ESCs migration, the 24-well transwell chambers (Corning, NY, USA) with 8-μm pores were used to assess the migration of EESCs. In brief, the transfected EESCs and NESCs were seeded into the upper chamber at 200 μL 2.5×10^4 cells density with DMEM/12F medium without serum, 700 μL DMEM/12F medium supplemented with 10 % FBS were added into lower chamber. After incubating for 48 h at 37 ℃ with 5 % CO2, the cells on the lower surface of membranes were fixed by 4% paraformaldehyde (Beyotime, Shanghai, China), stained by 0.1 % crystal violet (Beyotime, Shanghai, China) for 10 min. The images were obtained using BZ-X700 (Keyenth, Osaka city, Osaka Prefecture, Japan), and the number of cells migrated to independent areas was counted using Fiji software.

Measure of iron concentration

Intracellular iron concentrations were measured using an iron assay kit (ab83366, Abcam) according to manufacturer's instructions. Briefly, ESCs were lysed by Iron Assay Buffer (3×10^3 cells/well) in a final volume of 100 μL and treated with 5 μL Iron Reducer, plated in 96-well-plate and incubated at room temperature for 30 min. 100 μL iron probe was added to mark ferrous ion. The absorbance was measured at 593 nm with Multiskan SkyHigh (Thermofisher Scientific, Wilmington, DE, USA).

GSH and MDA content

Malondialdehyde (MDA) content in ESCs was assayed using a lipid peroxidation assay kit (ab118970, Abcam) after ADAMTS9-AS1 knockdown or overexpression in the presence or absence of miR-6516-5p or

siGpx4. Glutathione (GSH) content in ESCs was assayed using a Glutathione Assay Kit (ab65322, Abcam).

Lipid ROS level

Lipid ROS level was tested using a fluorescent-labelled oxidation sensitive probe (C11-BODIPY, Thermo Fisher Scientific) as previously described (30). In brief, ESCs (5×10^5) were plated in 24-well plates and treated with the indicated reagents. After 48 h, ESCs were treated with 1.5 μM of C11-BODIPY for 30 min at 37℃. Lipid ROS level was assessed using a flow cytometer (CytoFLEX, Beckman Coulter, FL, USA).

Western bolt

The protein extracted from ESCs lysate was quantified using the BCA Protein Assay Kit (Beyotime). Equal amounts of protein (approximate 50 μg) was loaded and separated on 12% SDS-PAGE for each experiment, then transferred to PVDF membranes (0.45 μm pore size; Millipore Corp., MA, USA). After blocking in 3% BSA at room temperature for 1 h, the membranes were treated with primary antibodies against GPX4 (1:4000, ab125066, Abcam, MA, USA) and β-actin (1:5000, ab8226, Abcam) for 18 h at 4°C, followed by incubation with HRP-conjured secondary antibody (HRP-labeled Goat Anti-Rabbit IgG(H+L); 1:5000; Beyotime) for 1.5 h. The bands were visualized using an ECL reagent (Beyotime) and quantified using Fiji software.

Fluorescence in situ hybridization (FISH)

The subcellular localization of ADAMTS9-AS1 was assessed with FISH Tag™ RNA Multicolor Kit (Carlsbad, CA, USA, USA). ESCs (3×10^4/well) were loaded on cover glasses, fixed with 4% paraformaldehyde (pH=7.4) for 5 min. After fixation, ESCs were digested by protease K (3 μg/mL) with glycine and acetic anhydride, followed by dehydrated in 75, 95, and 100% ethanol for 3 min each and air-dried at room temperature, and hybridization at 37 °C with probes (150 μL, 450 ng/mL) against ADAMTS9-AS1 for 48 h. Lastly, ESCs were stained by DAPI (Thermofisher Scientific) and observed under a fluorescence scanning microscope (BZ-X700; Keyenth, Osaka city, Osaka Prefecture, Japan).

Luciferase assay

The recombinant plasmids of pGL3-ADAMTS9-AS1 and pGL3-GPX4-3'UTR or their mutant were constructed in our laboratory by cloning approximate 350 bp cDNA into pGL3 vector (Vector Builder, Guangzhou, China). 4.5×10^4 ESCs were plated into 48-well plate and co-transfected with 70 nM of miR-6516-5p or miR-cont (used as control) with Lipofectamine™ 3000 (Invitrogen, Carlsbad, CA, USA). Luciferase activity was detected using the Renilla-Lumi™ Luciferase Reporter Gene Assay Kit (Beyotime, Shanghai, China) as the manufacturer's protocol.

RNA-pulldown assay

Biotin-labeled miR-6516-5p and miR-cont were transcribed *in vitro* using the Pierce™ Magnetic RNA-Protein Pull-Down Kit (Thermofisher Scientific, Wilmington, DE, USA). About 2×10^7 cells were dissolved in the standard lysis buffer (Thermofisher Scientific, Wilmington, DE, USA) plus 10 U/mL RNase Inhibitor (Beyotime, Shanghai, China). Next, each binding reaction was added streptavidin-labeled beads and incubated for 90 min. Lastly, ADAMTS9 AS1 in the eluate was quantified by q-PCR and GAPDH mRNA was used as a reference.

Statistical analysis

Data were analyzed using GraphPad 7.0 (GraphPad Software, La Jolla, CA, USA) and presented as mean ± SEM from at least three independent experiments. The significance between different groups was assessed using student *t* test or one-way ANOVA followed by Tukey-Kramer multiple comparisons test. P values lower than 0.05 was considered to indicate a statistically significant difference.

Results

ADAMTS9-AS1 expression was significantly up-regulated in ectopic endometrium (ecEM)

The expression level of ADAMTS9-AS1 is dys-regulated in ectopic endometrium (ecEM) (16) and in several type of cancer (15, 31, 32). To investigate the biological function of ADAMTS9-AS1 on EMs, the expression pattern of ADAMTS9-AS1 was verified in endometrial tissues. The data from qPCR analysis in seventeen paired ecEM and euEM tissues showed that the expression level of ADAMTS9-AS1 was significantly increased in ecEM compared to euEM (Figure 1A). To further validate the results, a murine model of EMs was established, and ecEM and euEM were collected. Figure 1B showed that the ADAMTS9-AS1 expression was also up-regulated in ecEM compared to euEM in murine model of EMs. Then the primary ectopic ESCs (EESCs) and normal ESCs (NESCs) were collected from ecEM and euEM, respectively, and the ADAMTS9-AS1 level was assessed. As shown in Figure 1C, the ADAMTS9-AS1 level in EESCs was higher than in NESCs.

ADAMTS9-AS1 accelerated ESCs growth and migration

To explore the effect of ADAMTS9-AS1 on regulating ESCs viability and migration, ADAMTS9-AS1 was knocked down in EESCs and overexpressed in NESCs (Supporting Figure S1A and B), respectively. Figure 2A showed that ADAMTS9-AS1 knockdown in EESCs significantly decreased cell viability. The results from FDA staining also revealed that ADAMTS9-AS1 knockdown resulted in a significant cell death (Figure 2B and C). Besides, the migratory behavior of ESCs acts as a crucial role in the EMs pathogenesis (33). Figure 2D and E showed that ADAMTS9-AS1 knockdown in EESCs significantly repressed cell migration. On the contrary, ADAMTS9-AS1 overexpression in NESCs increased cell viability (Figure 2F) and facilitated cell migration (Figure 2G and H). These data suggest that up-regulated ADAMTS9-AS1 increases ESCs viability and promotes ESCs migration.

ADAMTS9-AS1 repressed ferroptosis of ESCs

To investigate the pattern of ADAMTS9-AS1-induced ESCs cells death, EESCs were treated with ADAMTS9-AS1-specific siRNA (siADAMTS9-AS1) in the presence of Fer-1 (the specific inhibitor of ferroptosis), ZVAD-FMK (the specific inhibitor of apoptosis), 3-MA (the specific inhibitor of autophagy), or disulfiram (the specific inhibitor of pyroptosis). Forty-eight hours later cell viability was assessed using CCK-8. Figure 3A showed that siADAMTS9-AS1-decreasing EESCs viability was significantly prevented by Fer-1 and ZVAD-FMK, but not necrostatin-1, 3-MA and disulfiram, suggesting that ADAMTS9-AS1 knockdown accelerated EESCs death via triggering apoptosis and ferroptosis. In the study the role of ADAMTS9-AS1 in regulating ferroptosis of EESCs was explored because the effect of Fer-1 on regulating EESCs viability was more significant than ZVAD-FMK. Figure 3B further revealed that Erastin (the specific activator of ferroptosis) treatment decreased cell NESCs viability, whereas ADAMTS9-AS1 overexpression blocked the effect. Fer-1 also prevented sorafenib-induced EESCs death (Figure 3C). These data demonstrate that ferroptosis is an important form of ESCs death, and ADAMTS9-AS1 positively regulates ESCs death by ferroptosis pathway.

We then compared the ferroptosis level between NESCs and EESCs. Figure 4A-C showed that the iron concentration, MDA content, and ROS level were lower in EESCs than in NESCs, indicating that ferroptosis was repressed in EESCs. To define whether ADAMTS9-AS1 knockdown triggered ferroptosis of EESCs, ROS level and MDA content were assessed after ADAMTS9-AS1 knockdown. Figure 4D and E showed that ADAMTS9-AS1 inhibition resulted in significant increase of ROS and MDA level, suggesting that ADAMTS9-AS1 negatively regulated ferroptosis of EESCs. More important, ADAMTS9-AS1 inhibition significantly decreased the mRNA and protein expression of GPX4, a key repressor of ferroptosis (Figure 4F-H). These data indicate that ADAMTS9-AS1 negatively regulates ferroptosis of ESCs, possibly by regulating GPX4.

ADAMTS9-AS1 acted as a ceRNA through sponging miR-6516-5p

LncRNA located in cytoplasm commonly functions as ceRNA to indirectly control mRNA expression via absorbing miRNAs (34, 35). To explore the mechanism underlying ADAMTS9-AS1 in regulating ferroptosis, the subcellular localization of ADAMTS9-AS1 in ESCs was first assessed using FISH. As shown in Figure 5A, ADAMTS9-AS1 was primarily located in the cytoplasm in EESCs and NESCs. The bioinformatics tool (miRDB, http://mirdb.org/cgi-bin/search.cgi) (36) was used to predict the potential miRNAs absorbed by ADAMTS9-AS1. A total of 104 miRNAs were predicted through miRDB tool (Supporting Table S2). Based on the above results that ADAMTS9-AS1 positively regulated GPX4 expression, the miRNAs targeting GPX4 were screened using TargetScan 7.2 (http://www.targetscan.org/vert_72/). miR-6516-5p exhibited the potential to construct ADAMTS9-AS1/miR-6516-5p/GPX4 ceRNA networks (Figure 5B and F).

To assess the direct combination of ADAMTS9-AS1 with miR-6516-5p, the recombinant plasmids of pGL3-ADAMTS9-AS1 or pGL3-ADAMTS9-AS1-mut were transiently transfected into ESCs in the presence of miR-6516-5p. Figure 5C revealed that the luciferase activity of pGL3-ADAMTS9-AS1 was obviously reduced after co-transfection with miR-6516-5p compared with control (miR-cont), whereas miR-6516-5p

did not decrease the luciferase activity of pGL3-ADAMTS9-AS1-mut. Similarly, mutant miR-6516-5p did not affect the luciferase activity pGL3-ADAMTS9-AS1 (Figure 5D), indicating the specific combination of miR-6516-5p with ADAMTS9-AS1 by base-pair complementarity in the seed region of miR-6516-5p. RNA pull-down assay was used to further verify the direct binding of miR-6516-5p with ADAMTS9-AS1. Figure 5E revealed that ADAMTS9-AS1 was more enriched in the miR-6516-5p immunoprecipitates compared with miR-cont.

Based on the prediction that miR-6516-5p potentially targets GPX4 (Figure 5F), we next whether miR-6516-5p regulates GPX4 expression at the post-transcriptional level. To this end, the recombinant plasmids of pGL3-GPX4-3'UTR or pGL3-GPX4-3'UTR-mut were transfected into ESCs in the presence of miR-6516-5p. Figure 5G revealed that the luciferase activity of pGL3-GPX4-3'UTR was obviously reduced after co-transfection with miR-6516-5p compared with control (miR-cont), whereas miR-6516-5p did not decrease the luciferase activity of pGL3-GPX4-3'UTR-AS1-mut. Although miR-6516-5p overexpression (Supporting Figure S1C) could not inhibit GPX4 mRNA expression (data not shown), miR-6516-5p significantly repressed the protein expression of GPX4 (Figure 5H). Then the regulatory correlation of ADAMTS9-AS1 with miR-6516-5p, and GPX4 was explored. As shown in Figure 5I, the luciferase activity of pGL3-GPX4-3'UTR was decreased following miR-6516-5p overexpression, but the suppressive effect was destroyed in the presence of ADAMTS9-AS1, not ADAMTS9-AS1-Mut. These results demonstrate that ADAMTS9-AS1 competitively binds to miR-6516-5p with GPX4 and that ADAMTS9-AS1 might act as a ceRNA to regulate GPX4 expression by sponging miR-6516-5p.

ADAMTS9-AS1 increased GPX4 expression in miR-6516-5p-dependent manner

To verify whether ADAMTS9-AS1 functioned as a ceRNA to increase GPX4 expression by sponging miR-6516-5p, ADAMTS9-AS1 was overexpressed in ESCs in the presence or absence of miR-6516-5p and then the GPX4 expression was assessed using qPCR and western blot analysis. As shown in Figure 6A-C, forced expression of ADAMTS9-AS1 increased the mRNA and protein level of GPX4 in ESCs, whereas miR-6516-5p reversed the effect. Functionally, ADAMTS9-AS1 enhanced the proliferative and migratory ability of ESCs, whereas miR-6516-5p overexpression significantly inhibited the effect (Figure 6D-F). More important, ADAMTS9-AS1 decreased ROS level and MDA content, and increase GSH content, whereas miR-6516-5p overexpression or GPX4 knockdown significantly blocked the effect (Figure 7A-C), indicating that ADAMTS9-AS1 repressed ferroptosis in a miR-6516-5p/GPX4-dependent manner. Taken together, the present data demonstrate that ADAMTS9-AS1 accelerates EMs progression through repressing miR-6516-5p/GPX4-dependent ferroptosis of ESCs.

Discussion

Iron (Fe) is an indispensable element that regulates cell survival and proliferation, and it is reported that Fe shortage is correlated with many reproductive diseases (20). Paradoxically, Fe overload affects many respects involved in EMs progression including oxidative stress or lesion proliferation (37). As a Fe-dependent non non-apoptotic cell death, the biological role of ferroptosis in EMs is gradually being

revealed. Ferroptosis resistance is correlated with ESCs growth and proliferation, and ferroptosis-associated genes may possess a clinical potential in the diagnosis and treatment of EMs. In the present study, we demonstrate that, i) ADAMTS9-AS1 expression was significantly increased in ectopic endometrium, ii) ADAMTS9-AS1 accelerated ESCs growth and migration, iii) ADAMTS9-AS1 repressed ferroptosis of ESCs, iv) ADAMTS9-AS1 acted as a ceRNA through sponging miR-6516-5p, v) ADAMTS9-AS1 increased GPX4 expression in miR-6516-5p-dependent manner. These results demonstrated the important function of ADAMTS9-AS1/miR-6516-5p/GPX4/ferroptosis axis on regulating ESCs viability and migration, and may provide a potential opportunity to the therapy of EMs.

The role of ADAMTS9-AS1 in tumorigenesis and progression has been widely investigated. Through lncRNAs expression profiling analysis, Wang *et al*., first demonstrated that the ADAMTS9-AS1 level is significantly increased in epithelial ovarian cancer tissues compared normal tissues (38). ADAMTS9-AS1 overexpression represses prostate cancer cell proliferation, and low expression of ADAMTS9-AS1 predicts a poorer survival compared with higher ADAMTS9-AS1 expression, suggesting that ADAMTS9-AS1 functions as a tumor suppressive role in prostate cancer (15). On the contrary, ADAMTS9-AS1 facilitates cancer cell proliferation and migration in hepatocellular carcinoma and colorectal cancer (39, 40). These studies indicates that ADAMTS9-AS1 might exert differently biological effect in different type of cells. Especially, recent study showed that the ADAMTS9-AS1 expression is dys-regulated in ectopic endometrial tissues (16). Based on these facts, we investigated the biological role of ADAMTS9-AS1 in the pathogenesis of EMs. The current results revealed that the ADAMTS9-AS1 expression is significantly increased in ecEM compared with euEM in patients with EMs and in a murine model of EMs. Functional studies demonstrated that ADAMTS9-AS1 inhibition in ESCs represses cell viability and migration, whereas ADAMTS9-AS1 overexpression increases cell viability and migration, indicating that ADAMTS9-AS1 functions as an activator of EMs.

The underlying mechanism of ADAMTS9-AS1 on facilitating ESCs viability was further investigated. As an antisense lncRNAs, ADAMTS9-AS1 cannot affect the expression of overlapping coding genes (ADAMTS9, data not shown) (38), indicating that ADAMTS9-AS1 possesses other modes of function in EMs. Emerging studies demonstrated that lncRNA can interact with miRNA as a competing endogenous RNA (ceRNA) to regulate target mRNA (41). The ceRNA hypothesis has also been affirmed in EMs. Wang *et al*., identified an EMs-related ceRNA network involving forty-five pathways, and several ceRNAs as potential biomarkers for endometrial receptivity (42). LINC01541 sponges miR-506-5p to regulate its downstream Wnt/β-Catenin pathway in EMs, and thus inhibits the proliferation and invasion of ESCs (43). In the study we demonstrated that ADAMTS9-AS1 functions as a ceRNA via sponging miR-6516-5p to de-repress the expression of GPX4.

It is well known that GPX4 is the critical repressor of ferroptosis (44). As a glutathione-dependent enzyme, GPX4 converts toxic lipid hydroperoxides to non-toxic lipid alcohols (45), and thus decreases Fe-induced conversion of lipid hydroperoxides to highly reactive lipid alkoxy radicals. The genetic variants of *GPX4* are different between women with advanced stage EMs and mild EMs (46). Fox example, the GPX4 rs713041 is associated with the severity of EMs, indicating that the abnormity of GPX4 involves in the

pathogenesis of EMs. Moreover, the regulatory role of lncRNA in GPX4 expression has been verified. Bai *et al*., demonstrated that H19 knockdown decreases GPX4 expression and facilitates ferroptosis in spontaneous abortion (47). Based on these analysis, we investigated whether ADAMTS9-AS1 regulates ferroptosis resistance in EMs through miRNA/GPX4 axis. We demonstrated that ADAMTS9-AS1 accelerates ESCs proliferation and migration through regulating miR-6516-5p/GPX4-dependent ferroptosis.

Declarations

Acknowledgement

This work was supported by the Shanghai innovation pilot construction project of TCM diagnosis and treatment model (No. ZY(2018-2020)-FWTX-6006), the Project of Shanghai Health Bureau (NO.201840163), the Shinkang phase II three year action plan major clinical research program (No. SHDC2020CR4056), the Shanghai Committee of Science and Technology, China (20Y21901400), the Shanghai Committee of Science and Technology, China (20Z21900400), the Youth Project of Traditional Chinese Medicine Research Project of Shanghai Health (2020LQ001) and the Traditional Chinese Medicine Research Project of Shanghai Health (2020LP001).

Author contributions

CJ and SYH designed and supervised the project. WYT and GCC conducted experiments. KJY collected and analyzed the data. SJ wrote the manuscript. ZL edited the manuscript.

Conflicts of Interest

The authors declare no conflict of interest.

Data availability

All data generated or analysed during this study are included in this published article (and its Supplementary Information files).

References

1. Deiana D, Gessa S, Anardu M, et al.: Genetics of endometriosis: a comprehensive review. Gynecological endocrinology : the official journal of the International Society of Gynecological Endocrinology 35: 553-558, 2019.
2. Koninckx PR, Ussia A, Adamyan L, Wattiez A, Gomel V and Martin DC: Pathogenesis of endometriosis: the genetic/epigenetic theory. Fertility and sterility 111: 327-340, 2019.
3. Corachan A, Pellicer N, Pellicer A and Ferrero H: Novel therapeutic targets to improve IVF outcomes in endometriosis patients: a review and future prospects. Human reproduction update, 2021.

4. Horton J, Sterrenburg M, Lane S, Maheshwari A, Li TC and Cheong Y: Reproductive, obstetric, and perinatal outcomes of women with adenomyosis and endometriosis: a systematic review and meta-analysis. Human reproduction update 25: 592-632, 2019.
5. Ghafouri-Fard S, Shoorei H and Taheri M: Role of Non-coding RNAs in the Pathogenesis of Endometriosis. Frontiers in oncology 10: 1370, 2020.
6. Wang X, Zhang J, Liu X, Wei B and Zhan L: Long noncoding RNAs in endometriosis: Biological functions, expressions, and mechanisms. Journal of cellular physiology 236: 6-14, 2021.
7. Quinn JJ and Chang HY: Unique features of long non-coding RNA biogenesis and function. Nature reviews. Genetics 17: 47-62, 2016.
8. Kim SH, Lim KH, Yang S and Joo JY: Long non-coding RNAs in brain tumors: roles and potential as therapeutic targets. Journal of hematology & oncology 14: 77, 2021.
9. Keniry A, Oxley D, Monnier P, et al.: The H19 lincRNA is a developmental reservoir of miR-675 that suppresses growth and Igf1r. Nature cell biology 14: 659-665, 2012.
10. da Rocha ST and Heard E: Novel players in X inactivation: insights into Xist-mediated gene silencing and chromosome conformation. Nature structural & molecular biology 24: 197-204, 2017.
11. Grote P, Wittler L, Hendrix D, et al.: The tissue-specific lncRNA Fendrr is an essential regulator of heart and body wall development in the mouse. Developmental cell 24: 206-214, 2013.
12. Xu J, Qian Y, Ye M, et al.: Distinct expression profile of lncRNA in endometrial carcinoma. Oncology reports 36: 3405-3412, 2016.
13. Zhou C, Zhang T, Liu F, et al.: The differential expression of mRNAs and long noncoding RNAs between ectopic and eutopic endometria provides new insights into adenomyosis. Molecular bioSystems 12: 362-370, 2016.
14. Zhang C, Wu W, Zhu H, et al.: Knockdown of long noncoding RNA CCDC144NL-AS1 attenuates migration and invasion phenotypes in endometrial stromal cells from endometriosisdagger. Biology of reproduction 100: 939-949, 2019.
15. Wan J, Jiang S, Jiang Y, et al.: Data Mining and Expression Analysis of Differential lncRNA ADAMTS9-AS1 in Prostate Cancer. Frontiers in genetics 10: 1377, 2019.
16. Cui L, Chen S, Wang D and Yang Q: LINC01116 promotes proliferation and migration of endometrial stromal cells by targeting FOXP1 via sponging miR-9-5p in endometriosis. Journal of cellular and molecular medicine 25: 2000-2012, 2021.
17. Hirschhorn T and Stockwell BR: The development of the concept of ferroptosis. Free radical biology & medicine 133: 130-143, 2019.
18. Dixon SJ, Lemberg KM, Lamprecht MR, et al.: Ferroptosis: an iron-dependent form of nonapoptotic cell death. Cell 149: 1060-1072, 2012.
19. Stockwell BR, Friedmann Angeli JP, Bayir H, et al.: Ferroptosis: A Regulated Cell Death Nexus Linking Metabolism, Redox Biology, and Disease. Cell 171: 273-285, 2017.

20. Ng SW, Norwitz SG, Taylor HS and Norwitz ER: Endometriosis: The Role of Iron Overload and Ferroptosis. Reprod Sci 27: 1383-1390, 2020.
21. Dixon SJ and Stockwell BR: The role of iron and reactive oxygen species in cell death. Nature chemical biology 10: 9-17, 2014.
22. Xie Y, Hou W, Song X, et al.: Ferroptosis: process and function. Cell death and differentiation 23: 369-379, 2016.
23. Murphy AA, Santanam N, Morales AJ and Parthasarathy S: Lysophosphatidyl choline, a chemotactic factor for monocytes/T-lymphocytes is elevated in endometriosis. The Journal of clinical endocrinology and metabolism 83: 2110-2113, 1998.
24. Arumugam K and Yip YC: De novo formation of adhesions in endometriosis: the role of iron and free radical reactions. Fertility and sterility 64: 62-64, 1995.
25. Lousse JC, Defrere S, Van Langendonckt A, et al.: Iron storage is significantly increased in peritoneal macrophages of endometriosis patients and correlates with iron overload in peritoneal fluid. Fertility and sterility 91: 1668-1675, 2009.
26. Mashima T, Iwasaki R, Kawata N, et al.: In silico chemical screening identifies epidermal growth factor receptor as a therapeutic target of drug-tolerant CD44v9-positive gastric cancer cells. British journal of cancer 121: 846-856, 2019.
27. Mariani M, Vigano P, Gentilini D, et al.: The selective vitamin D receptor agonist, elocalcitol, reduces endometriosis development in a mouse model by inhibiting peritoneal inflammation. Human reproduction 27: 2010-2019, 2012.
28. Kato T, Yasuda K, Matsushita K, et al.: Interleukin-1/-33 Signaling Pathways as Therapeutic Targets for Endometriosis. Frontiers in immunology 10: 2021, 2019.
29. Somigliana E, Vigano P, Rossi G, Carinelli S, Vignali M and Panina-Bordignon P: Endometrial ability to implant in ectopic sites can be prevented by interleukin-12 in a murine model of endometriosis. Human reproduction 14: 2944-2950, 1999.
30. Zhu Y, Zhang C, Huang M, Lin J, Fan X and Ni T: TRIM26 Induces Ferroptosis to Inhibit Hepatic Stellate Cell Activation and Mitigate Liver Fibrosis Through Mediating SLC7A11 Ubiquitination. Frontiers in cell and developmental biology 9: 644901, 2021.
31. Wang J, Zhang C, Wu Y, He W and Gou X: Identification and analysis of long non-coding RNA related miRNA sponge regulatory network in bladder urothelial carcinoma. Cancer cell international 19: 327, 2019.
32. Li N, Li J, Mi Q, et al.: Long non-coding RNA ADAMTS9-AS1 suppresses colorectal cancer by inhibiting the Wnt/beta-catenin signalling pathway and is a potential diagnostic biomarker. Journal of cellular and molecular medicine 24: 11318-11329, 2020.
33. Gentilini D, Vigano P, Somigliana E, et al.: Endometrial stromal cells from women with endometriosis reveal peculiar migratory behavior in response to ovarian steroids. Fertility and sterility 93: 706-715, 2010.

34. Thomson DW and Dinger ME: Endogenous microRNA sponges: evidence and controversy. Nature reviews. Genetics 17: 272-283, 2016.
35. Bai J, Wang B, Wang T and Ren W: Identification of Functional lncRNAs Associated With Ovarian Endometriosis Based on a ceRNA Network. Frontiers in genetics 12: 534054, 2021.
36. Wong N and Wang X: miRDB: an online resource for microRNA target prediction and functional annotations. Nucleic acids research 43: D146-152, 2015.
37. Defrere S, Lousse JC, Gonzalez-Ramos R, Colette S, Donnez J and Van Langendonckt A: Potential involvement of iron in the pathogenesis of peritoneal endometriosis. Molecular human reproduction 14: 377-385, 2008.
38. Wang H, Fu Z, Dai C, et al.: LncRNAs expression profiling in normal ovary, benign ovarian cyst and malignant epithelial ovarian cancer. Scientific reports 6: 38983, 2016.
39. Zhang Z, Li H, Hu Y and Wang F: Long non-coding RNA ADAMTS9-AS1 exacerbates cell proliferation, migration, and invasion via triggering of the PI3K/AKT/mTOR pathway in hepatocellular carcinoma cells. American journal of translational research 12: 5696-5707, 2020.
40. Chen W, Tu Q, Yu L, et al.: LncRNA ADAMTS9-AS1, as prognostic marker, promotes cell proliferation and EMT in colorectal cancer. Human cell 33: 1133-1141, 2020.
41. Salmena L, Poliseno L, Tay Y, Kats L and Pandolfi PP: A ceRNA hypothesis: the Rosetta Stone of a hidden RNA language? Cell 146: 353-358, 2011.
42. Wang X and Yu Q: Endometriosis-related ceRNA network to identify predictive biomarkers of endometrial receptivity. Epigenomics 11: 147-167, 2019.
43. Mai H, Xu H, Lin H, et al.: LINC01541 Functions as a ceRNA to Modulate the Wnt/beta-Catenin Pathway by Decoying miR-506-5p in Endometriosis. Reprod Sci 28: 665-674, 2021.
44. Chen X, Yu C, Kang R, Kroemer G and Tang D: Cellular degradation systems in ferroptosis. Cell death and differentiation 28: 1135-1148, 2021.
45. Cao JY and Dixon SJ: Mechanisms of ferroptosis. Cellular and molecular life sciences : CMLS 73: 2195-2209, 2016.
46. Huang YY, Wu CH, Liu CH, et al.: Association between the Genetic Variants of Glutathione Peroxidase 4 and Severity of Endometriosis. International journal of environmental research and public health 17, 2020.
47. Bai RX and Tang ZY: Long non-coding RNA H19 regulates Bcl-2, Bax and phospholipid hydroperoxide glutathione peroxidase expression in spontaneous abortion. Experimental and therapeutic medicine 21: 41, 2021.

Figures

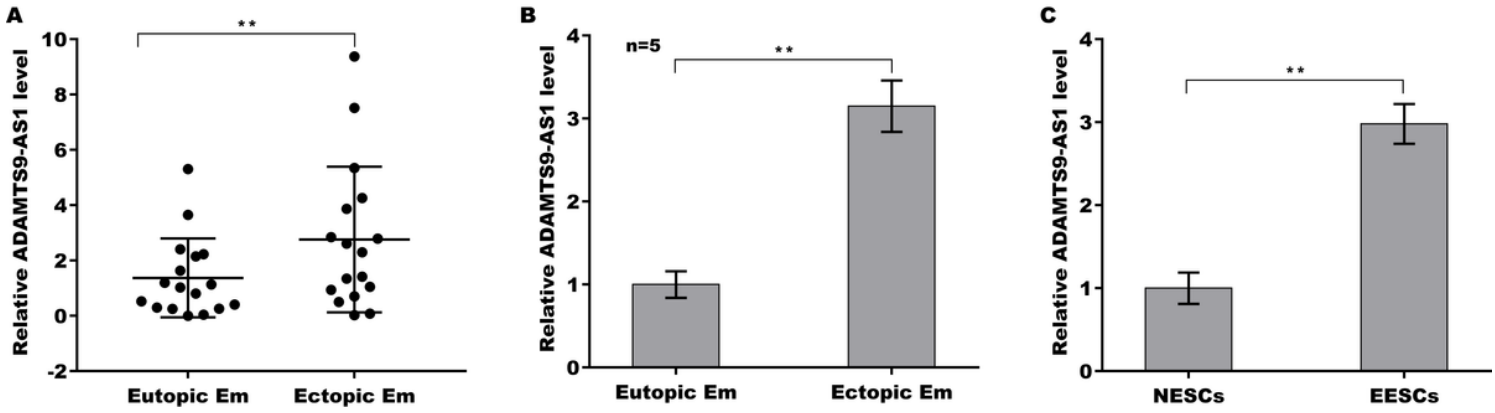

Figure 1

ADAMTS9-AS1 expression was increased in ectopic EM. (A) qPCR analysis of ADAMTS9-AS1 in paired ectopic EM and eutopic EM tissues (n=17) in women with EMs. (B) A murine model of EMs was established and the expression level of ADAMTS9-AS1 was assessed using qPCR analysis in ectopic EM and eutopic EM tissues (n=5). (C) The primary ectopic ESCs (EESCs) and normal ESCs (NESCs) were isolated from ectopic EM and eutopic EM of EMs mice, respectively, and then the ADAMTS9-AS1 level was assessed using qPCR analysis (n=5). **p<0.01.

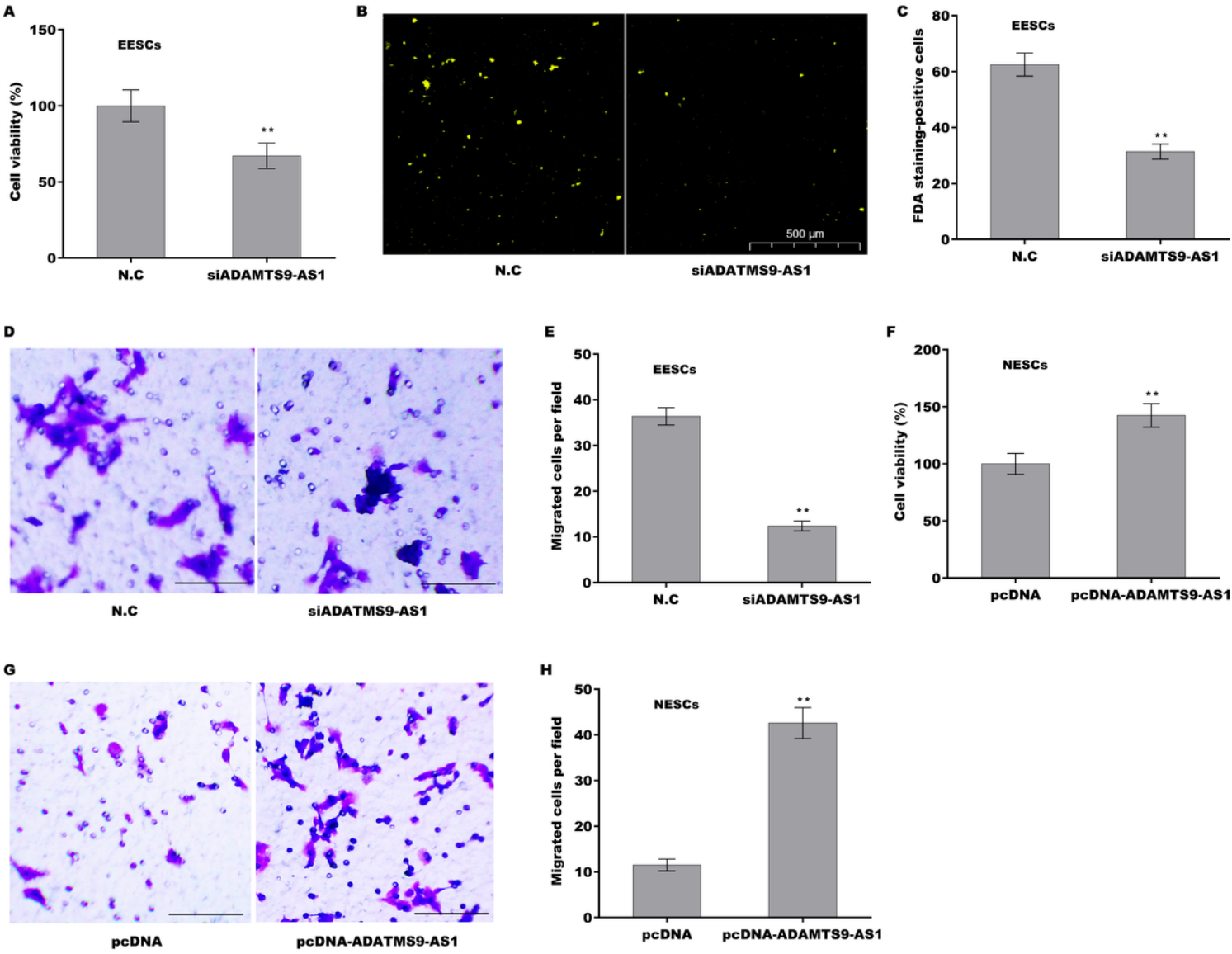

Figure 2

ADAMTS9-AS1 facilitated ESCs growth and migration. (A) Cell viability of EESCs after ADAMTS9-AS1 knockdown was assessed using CCK-8 assay. (B and C) Cell viability of EESCs after ADAMTS9-AS1 knockdown was assessed using FDA staining. (D and E) Cell migration of EESCs after ADAMTS9-AS1 knockdown was assessed using transwell migration assay. (F) Cell viability of NESCs after ADAMTS9-AS1 overexpression was assessed using CCK-8 assay. (G and H) Cell migration of NESCs after ADAMTS9-AS1 overexpression was assessed using transwell migration assay. **p<0.01.

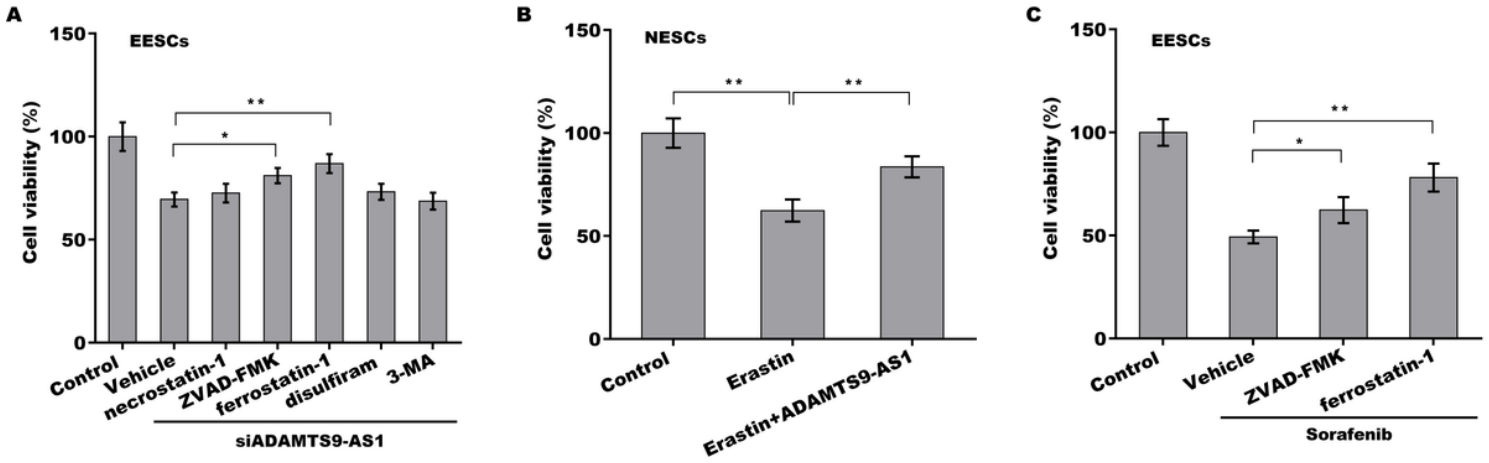

Figure 3

ADAMTS9-AS1 increased ESCs viability by regulating ferroptosis. (A) Cell viability of EESCs was assessed after ADAMTS9-AS1 knockdown using CCK-8 assay in the presence of the indicated inhibitors (ZVAD-FMK, 10 μM; necrostatin-1, 10μM; ferrostatin-1, 1μM; disulfiram, 5μM; 3-MA, 10mM). (B) Cell viability of NESCs was assessed after ADAMTS9-AS1 overexpression using CCK-8 assay in the presence or absence of Erastin (10μM). (C) Cell viability of EESCs was assessed after treatment with the indicated inhibitors (ZVAD-FMK, 10μM; ferrostatin-1, 1μM) in the presence or absence of Sorafenib (5μM). $p<0.05$, $^{**}p<0.01$.

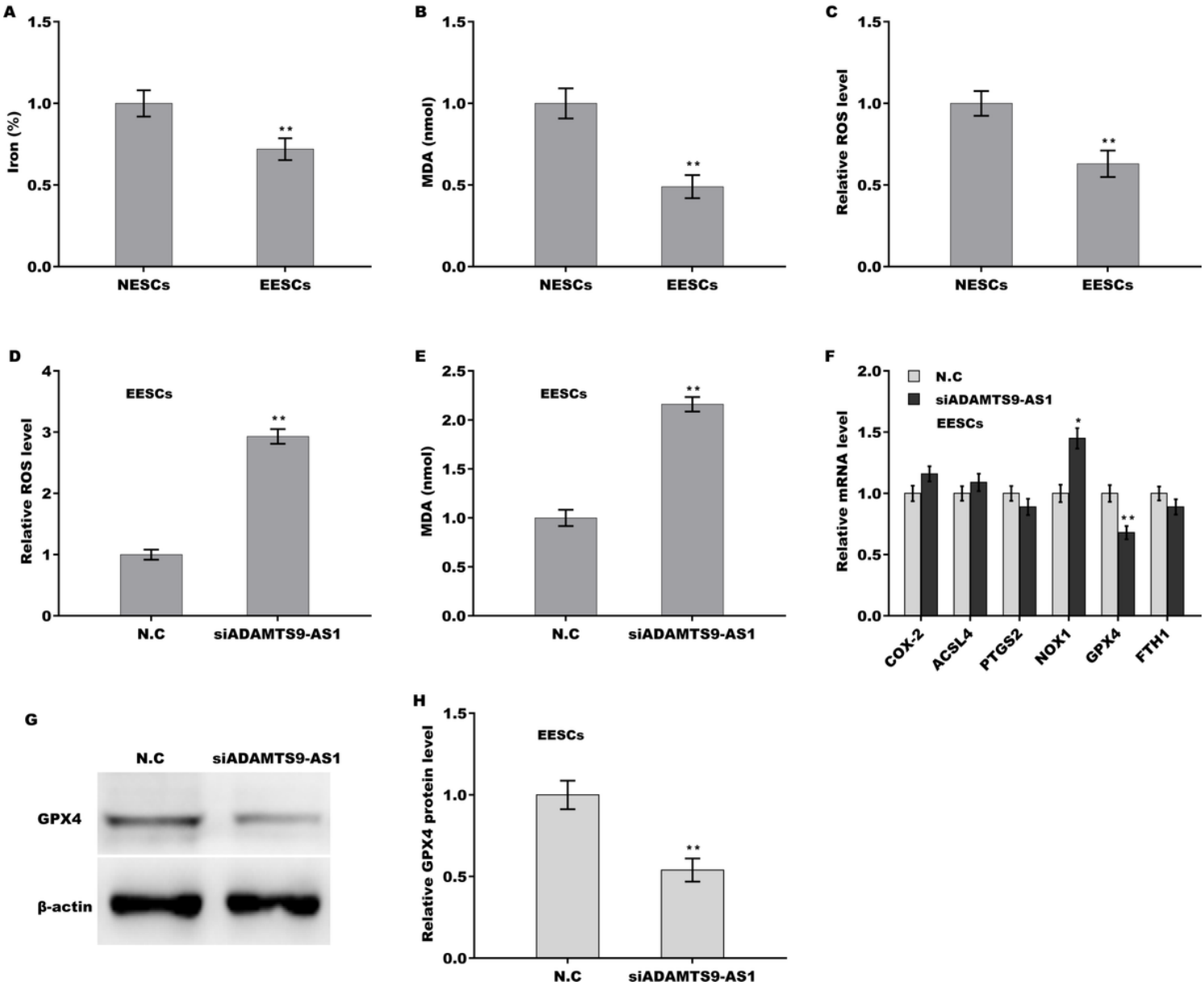

Figure 4

ADAMTS9-AS1 repressed ferroptosis of ESCs by regulating GPX4. The levels of Fe2+ (A) and MDA content (B), and ROS levels (C) were assayed using the indicated kits in NESCs and EESCs. The levels of ROS (D) and MDA content (E) were assessed using the indicated kits in EESCs after ADAMTS9-AS1 knockdown. (F) The mRNA levels of COX-2, ACSL4, PTGS2, NOX1, GPX4, and FTH1 were assayed using qPCR analysis in EESCs after ADAMTS9-AS1 knockdown. (G and H) The protein level of GPX4 was assayed using western blot analysis in EESCs after ADAMTS9-AS1 knockdown. *p<0.05, **p<0.01.

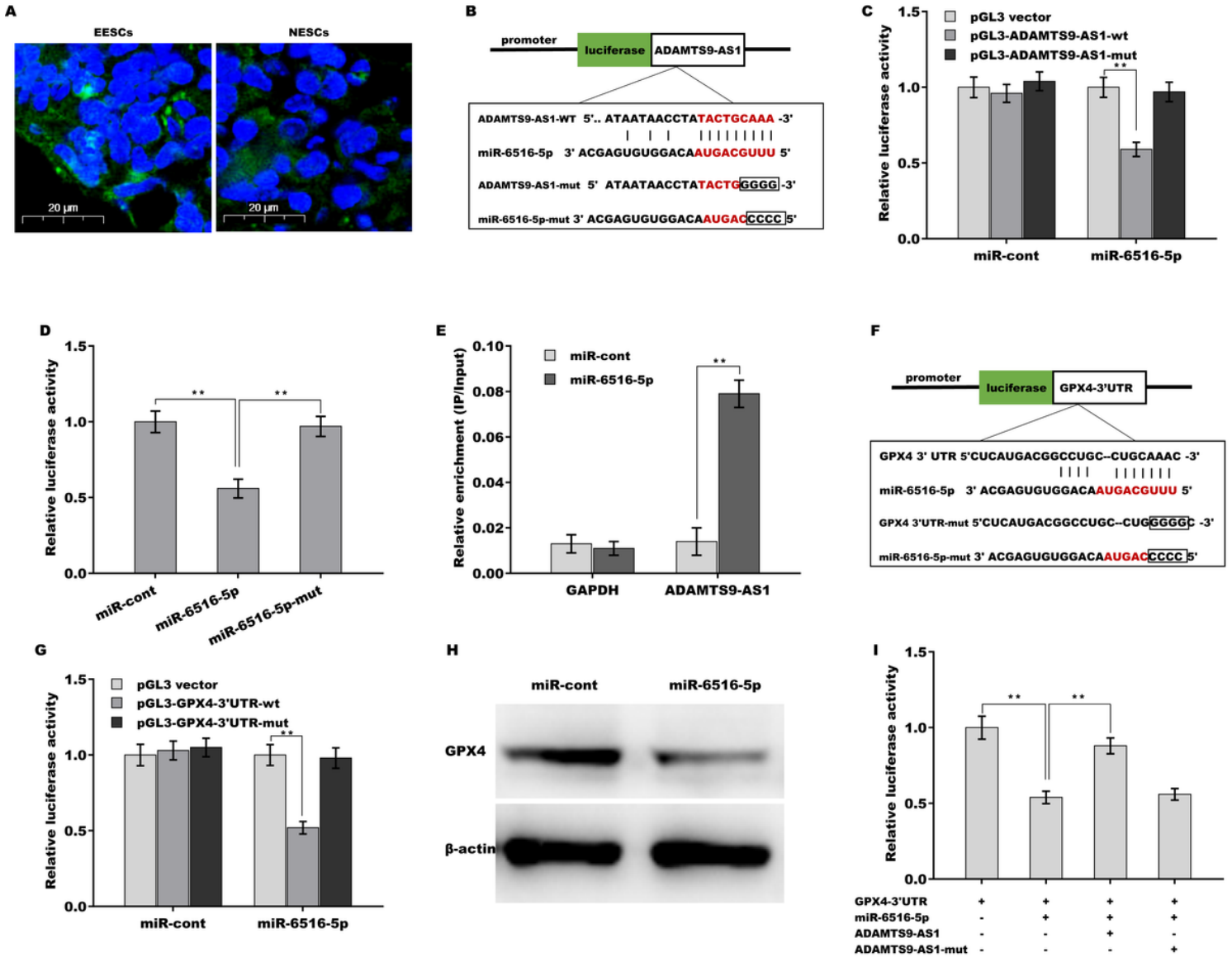

Figure 5

ADAMTS9-AS1 acted as a ceRNA through sponging miR-6516-5p. (A) The sub-cellular localization of ADAMTS9-AS1 in EESCs and NESCs was analyzed using RNA-FISH assay. Probes targeting ADAMTS9-AS1 were stained in green and DAPI was used to stain the nucleus of EESCs and NESCs. (B) Schematic representation of predicted binding sites of miR-6516-5p in ADAMTS9-AS1 sequence. (C) Luciferase activity was assessed using dual luciferase reporter assay in ESCs co-transfected with miR-6516-5p and recombinant luciferase reporter plasmids containing ADAMTS9-AS-wt (or ADAMTS9-AS-mut). Renilla luciferase was used as the internal control for normalizing transfection efficiency, and data are showed as the relative ratio of firefly luciferase activity. (D) Luciferase activity was assessed using dual luciferase reporter assay in ESCs co-transfected with miR-6516-5p (or miR-6516-5p-mut or miRcont) and recombinant luciferase reporter plasmids containing ADAMTS9-AS-wt. (E) The direct combination of ADAMTS9-AS with miR-6516-5p was assessed through RNA pull-down assay using 3'-biotinylated miR-6516-5p as bait. (F) Schematic representation of predicted binding sites of miR-6516-5p in GPX4-3'UTR sequence. (G) Luciferase activity was assessed using dual luciferase reporter assay in ESCs co-

transfected with miR-6516-5p (or miRcont) and recombinant luciferase reporter plasmids containing GPX4-3'UTR-wt (or GPX4-3'UTR-mut). (H) The protein expression of GPX4 was assessed using western blot analysis in ESCs after miR-6516-5p overexpression. (I) Luciferase activity was assessed using dual luciferase reporter assay in ESCs co-transfected with miR-6516-5p and luciferase reporters containing GPX4-3'UTR, ADAMTS9-AS-wt, or ADAMTS9-AS-Mut. *p<0.05, **p<0.01.

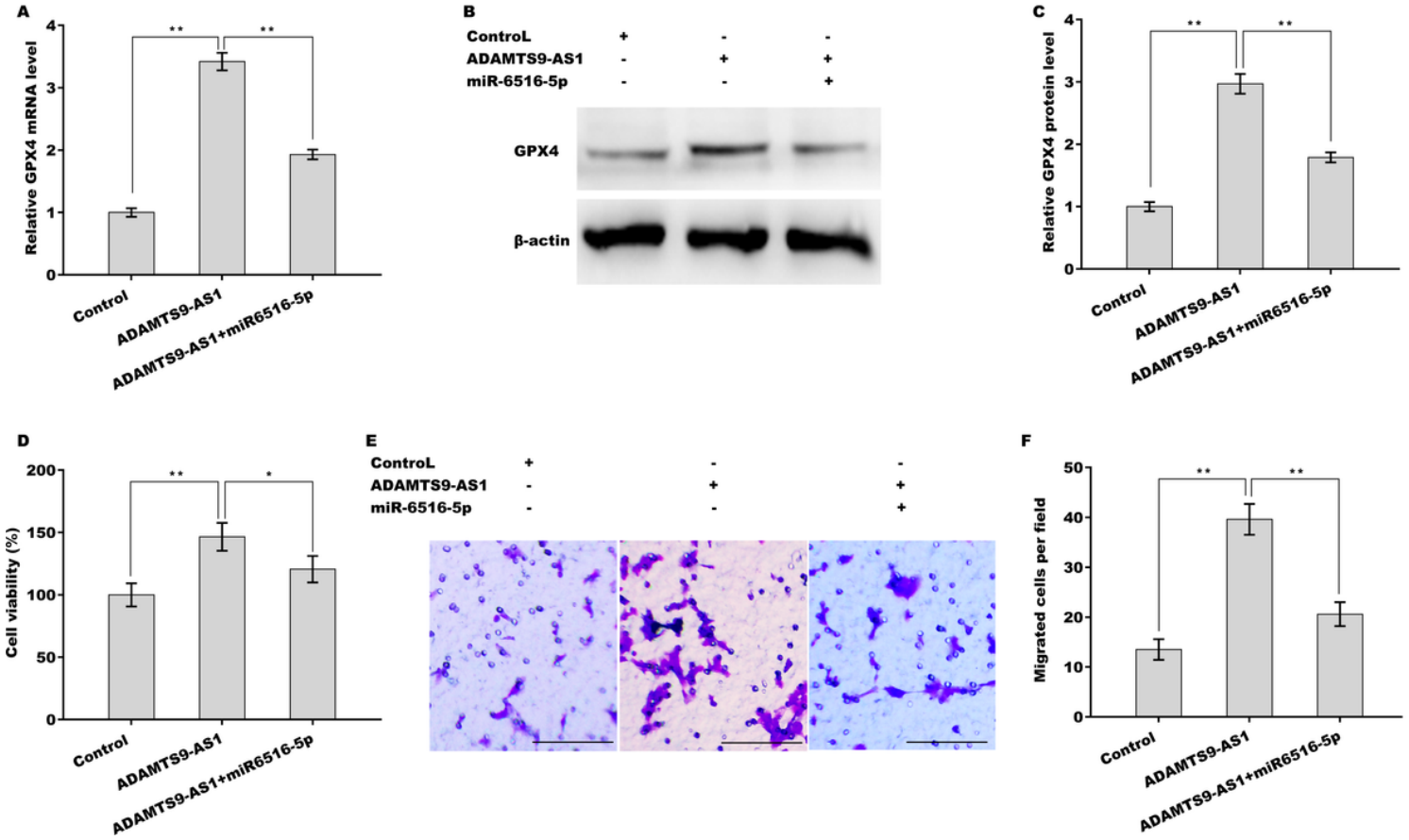

Figure 6

ADAMTS9-AS1 increased GPX4 expression in miR-6516-5p-dependent manner. qPCR (A) and western blot analysis (B and C) of GPX4 expression in ESCs after overexpression with ADAMTS9-AS1 in the presence or absence of miR-6516-5p. (D) ESCs viability was assessed using CCK-8 assay after overexpression with ADAMTS9-AS1 in the presence or absence of miR-6516-5p. (E and F) ESCs migration was assessed using transwell migration assay after overexpression with ADAMTS9-AS1 in the presence or absence of miR-6516-5p. *p<0.05. **p<0.01.

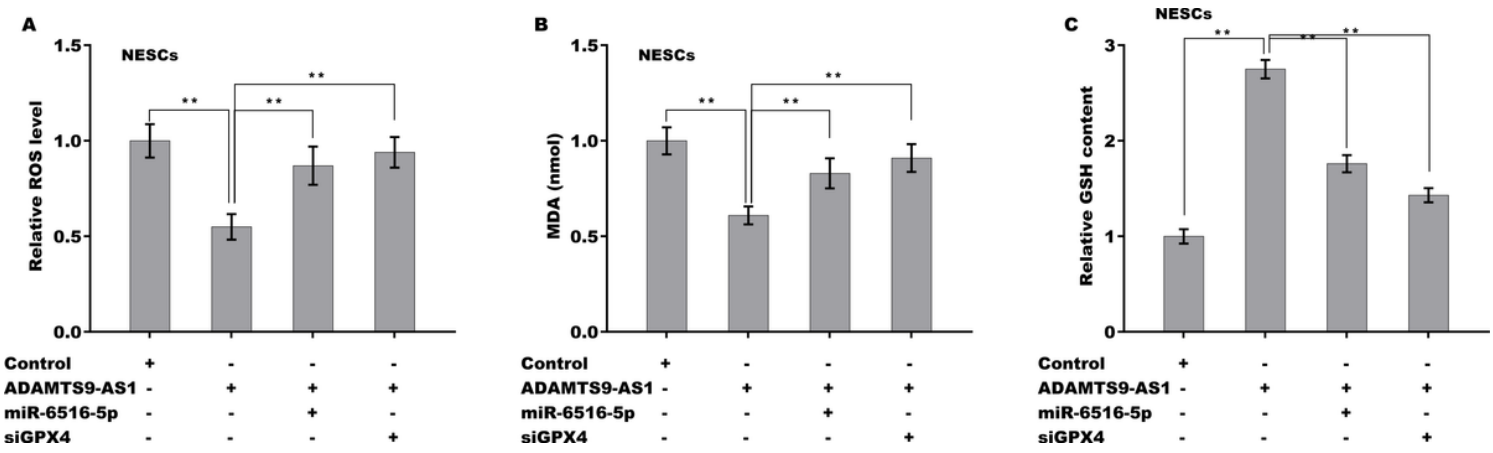

Figure 7

The effect of ADAMTS9-AS1/miR-6516-5p/GPX4 axis on ferroptosis. The ROS levels (A), MDA content (B), and GSH content (C) were assessed in NESCs after ADAMTS9-AS1 overexpression in the presence or absence of miR-6516-5p or siRNA-Gpx4. **p<0.01.

Supplementary Files

This is a list of supplementary files associated with this preprint. Click to download.

- SupportingFigureS1.tif
- SupportingTableS1.docx
- SupportingTableS2.docx